Physics Letters B 740 (2015) 243–249

Contents lists available at ScienceDirect

Physics Letters B

www.elsevier.com/locate/physletb

High-spin states beyond the proton drip-line: Quasiparticle alignments in ^{113}Cs

P.T. Wady [a,b], J.F. Smith [a,b,*], B. Hadinia [a,b,1], D.M. Cullen [c], S.J. Freeman [c], I.G. Darby [d,2], S. Eeckhaudt [e], T. Grahn [e], P.T. Greenlees [e], P.M. Jones [e,3], R. Julin [e], S. Juutinen [e], H. Kettunen [e], M. Leino [e], A.-P. Leppänen [e], B.M. McGuirk [d], P. Nieminen [e], M. Nyman [e], R.D. Page [d], J. Pakarinen [e], E.S. Paul [d], P. Rahkila [e], S.V. Rigby [c], C. Scholey [e], J. Uusitalo [e], R. Wadsworth [f]

[a] School of Engineering, University of the West of Scotland, Paisley, PA1 2BE, United Kingdom
[b] Scottish Universities Physics Alliance, United Kingdom
[c] School of Physics and Astronomy, University of Manchester, Manchester, M13 9PL, United Kingdom
[d] Department of Physics, Oliver Lodge Laboratory, University of Liverpool, Liverpool, L69 7ZE, United Kingdom
[e] Department of Physics, University of Jyväskylä, FIN-40014, Jyväskylä, Finland
[f] Department of Physics, University of York, Heslington, YO10 5DD, United Kingdom

ARTICLE INFO

Article history:
Received 28 June 2014
Received in revised form 11 November 2014
Accepted 22 November 2014
Available online 26 November 2014
Editor: V. Metag

Keywords:
Proton decay
Recoil-decay tagging
Gamma-ray spectroscopy
High-spin states
Quasiparticle alignments

ABSTRACT

Excited states have been studied in the deformed proton emitter ^{113}Cs. Gamma-ray transitions have been unambiguously assigned to ^{113}Cs by correlation with its characteristic proton decay, using the method of recoil-decay tagging. Two previously identified rotational bands have been observed and extended to tentative spins of 45/2 and 51/2 $\hbar$, with excitation energies over 8 MeV above the lowest state. These are the highest angular momenta and excitation energies observed to date in any nucleus beyond the proton drip-line. Transitions in the bands have been rearranged compared to previous work. A study of aligned angular momenta, in comparison to the predictions of Woods–Saxon cranking calculations, is consistent with the most intense band being based on the $\pi g_{7/2}[422]3/2^+$ configuration, which would contradict the earlier $\pi h_{11/2}$ assignment, and with the second band being based on the $\pi d_{5/2}[420]1/2^+$ configuration. The data suggest that the band based upon the $\pi h_{11/2}$ configuration is not observed.

Four decades ago, mass calculations suggested that the very neutron-deficient $Z = 55$ isotope ^{113}Cs would be unstable against proton emission. A number of experimental searches for this new type of decay ensued [1–3], leading to the establishment of proton radioactivity in this nucleus by Faestermann et al. in 1984 [4]. Being one of the first proton emitters identified, ^{113}Cs has become a nucleus of considerable interest in this field of study. Since the first work, the ground-state proton decay of ^{113}Cs has been the focus of several experiments [5–7] with the most recent studies giving decay properties of $T_{1/2} = 16.7(7)$ μs [7] and $E_p = 959(6)$ keV [6]. In the past 15 years, such characteristic proton decays have been exploited in γ-ray spectroscopy experiments using the technique known as recoil-decay tagging (RDT), in which prompt γ rays emitted at a reaction site are tagged using spatial and temporal correlations of the decay of reaction products that have been transported to the focal plane of a recoil spectrometer [8–10]. The RDT technique has recently been demonstrated to work with cross-sections down to at least tens of nanobarns [11]. The production cross-section for ^{113}Cs is around three orders of magnitude larger than this value, rendering it an ideal case for detailed spectroscopy at the proton drip-line using RDT. A study of rotational excitations in ^{113}Cs will allow the extraction of properties such as quasiparticle alignment frequencies and moments of inertia, which can be used to characterize intrinsic states and infer structural information.

* Corresponding author at: School of Engineering, University of the West of Scotland, Paisley Campus, Paisley, PA1 2BE Scotland, UK. Tel.: +44 141 848 3652; fax: +44 141 848 3663.
E-mail address: John.F.Smith@uws.ac.uk (J.F. Smith).
[1] Present address: Department of Physics, University of Guelph, Guelph, Ontario, N1G 2W1, Canada.
[2] Present address: Department of Nuclear Sciences and Applications, International Atomic Energy Agency, A-1400 Vienna, Austria.
[3] Present address: iThemba LABS, P.O. Box 722, Somerset West 7129, South Africa.

http://dx.doi.org/10.1016/j.physletb.2014.11.045

The odd-A neutron-deficient cesium isotopes with $A \geq 121$ ($N \geq 66$) have been comprehensively studied in γ-ray spectroscopy experiments [12–17]. Below $A = 121$, the isotopes ^{117,119}Cs have been studied in a high-spin, high-statistics γ-ray spectroscopy experiment, revealing a number of rotational bands based on $\pi h_{11/2}$, $\pi g_{7/2}$, and $\pi g_{9/2}^{-1}$ orbitals: ten bands were observed in ^{119}Cs [18] extending to $95/2\ \hbar$, and three bands were observed in ^{117}Cs [19] extending to $71/2\ \hbar$. Moving closer to the proton drip-line, γ-ray spectroscopy becomes increasingly more challenging. The best way to produce these nuclei is to use heavy-ion fusion–evaporation, but such reactions often require neutron evaporation from compound nuclei which are themselves very neutron deficient. Consequently, charged-particle evaporation dominates, and production cross-sections for nuclei near and at the proton drip-line are small, against a high background of more prolific channels. Although the ground-state decay of the $N = 60$ isotope ^{115}Cs has been identified [2], to date, no excited states have been reported; RDT cannot be used to study this nucleus as it does not decay by proton or α-particle emission, and its production cross section is very small, rendering in-beam γ-ray spectroscopy very difficult. The $N = 58$ isotope ^{113}Cs has, however, been the subject of two previous γ-ray spectroscopy experiments. Both experiments used the RDT technique applied to the ^{58}Ni(^{58}Ni, $2pn$) reaction, at a beam energy of 230 MeV, for which the cross-section was reported to be around 5 μb. In the first experiment, Gross et al. [20] identified four γ-ray transitions, which were tentatively assigned to be the yrast $\pi h_{11/2}$ band. In the second experiment, Yu et al. [21] observed two rotational bands, each consisting of eight transitions, which were assigned to be based on $\pi h_{11/2}$ and $\pi g_{7/2}$ orbitals. In the present work, an experiment has been carried out at the Accelerator Laboratory of the University of Jyväskylä, using the RDT method to further study the excited states of ^{113}Cs. Transitions in the two previously observed bands have been rearranged and new γ rays have been observed, allowing extension of the bands up to tentative spins of $45/2$ and $51/2\ \hbar$.

The reaction chosen for the present work was the same as that used in Refs. [20,21]. The beam of ^{58}Ni ions, with energy 230 MeV and intensity ∼1.5 pnA, was provided by the K130 cyclotron at the University of Jyväskylä Accelerator Laboratory, and was incident upon a 500-μg/cm^2 ^{58}Ni target. Prompt γ rays, emitted at the reaction site, were detected by the Jurogam γ-ray spectrometer, consisting of 42 Eurogam Phase-I-type [22], Compton-suppressed HPGe detectors with a total detection efficiency of 4.2%. Recoiling reaction products were separated from the primary beam by the RITU gas-filled recoil separator [23]. On exit from RITU, the reaction products passed through a multi-wire proportional counter (MWPC) before being implanted into double-sided silicon strip detectors (DSSDs); the MWPC and DSSDs were part of the GREAT spectrometer [24]. Data were recorded using the total-data-readout data-acquisition system [25] in which a 100-MHz clock was used, providing a timestamp on each detector signal, accurate to the nearest 10 ns. In total, ∼390 GB of data were recorded, consisting of 1.2×10^9 prompt γ rays, 1.6×10^9 DSSD implants (in time correlation with MWPC), and 2.4×10^8 DSSD decays (no MWPC correlation).

For the prompt γ-ray data, a software γ-ray coincidence window of 70 ns was applied, resulting in a mean γ-ray fold of 1.4 and a total of 7×10^8 $\gamma\gamma$ events. Examination of a recoil-gated $\gamma\gamma$ matrix revealed the dominant evaporation residues to be ^{112}Te ($4p$ evaporation; 50%), ^{113}I ($3p$; 40%), ^{112}I ($3pn$; 3%) and ^{114}Xe ($2p$; 3%), with other products, including ^{113}Cs, making up just a few percent of the total prompt γ-ray yield. Characteristic decay energies and half-lives of nuclei implanted in the DSSD allowed further identification: proton decays of ^{112,113}Cs and ^{109}I were observed, along with α decays of ^{108,109}Te and ^{110}I. Transitions in ^{113}I [26] and ^{113}Xe [27] were also observed due to β-delayed proton emission.

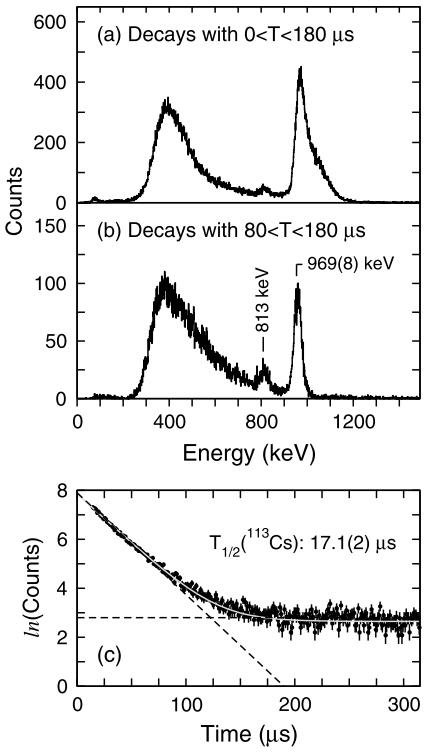

Fig. 1. Panels (a) and (b) show energy spectra from the DSSD. Panel (a) gives the spectrum of decays recorded within 180 μs of an implant. The large peak at ∼1 MeV is attributed to ^{113}Cs proton decays; the high-energy tail on the peak is due to pile-up of fast decays with the tail of the implant signal. Panel (b) shows decays recorded between 80 and 180 μs after an implant; the pile-up tail is no longer present, allowing the position of the proton-decay peak to be determined to be 969(8) keV. Also apparent on panels (a) and (b) is the peak at 813 keV due to proton decays of ^{109}I ($T_{1/2} \simeq 100$ μs) and ^{112}Cs ($T_{1/2} \simeq 500$ μs). Panel (c) gives the time between implant and decay in the DSSD, gated on the 969-keV peak; the data give a half-life of 17.1(2) μs.

An energy spectrum of decay products recorded in the DSSD within 180 μs of an implant is shown in Fig. 1(a). The peak in the spectrum at ∼1 MeV is attributed to ^{113}Cs proton decays. This peak has a high-energy tail extending to ∼1.2 MeV, which is due to fast decays (within several μs) piling-up with the tail of the most recent implant. Fig. 1(b) shows the same spectrum but with the condition that the decay must occur between 80 and 180 μs after an implant; the tail on the peak is no longer present and a measurement of the decay energy can then be made. The energy calibration of the DSSD was carried out using the ^{109}I proton-decay peak at 813(4) keV [28] along with α-decay peaks for ^{108,109}Te and ^{110}I [29], with energies between 3.0 and 3.5 MeV. The ^{113}Cs proton decay energy was then found to be 969(8) keV, which is close to previous measurements, such as that in Ref. [6]. Decay times, gated on the 969-keV peak, are shown in Fig. 1(c). A fit to the first 80 μs with a flat baseline subtraction applied gives the half-life to be 17.1(2) μs, which is in good agreement with value of 17(2) μs reported in Ref. [6] and that of 16.7(7) μs from Ref. [7], but lower than the value of 33(7) μs from Ref. [5]. In total, approximately 18 000 ^{113}Cs proton decays were observed. A consideration of beam intensity, target thickness, and detection efficiencies suggests that the production cross-section of ^{113}Cs is 20(10) μb, cf. 5 μb reported in Refs. [20,21].

The total projection of a $\gamma\gamma$ matrix incremented without selective gates is shown in Fig. 2(a). The majority of the peaks in the spectrum correspond to transitions in ^{112}Te and ^{112,113}I. Following

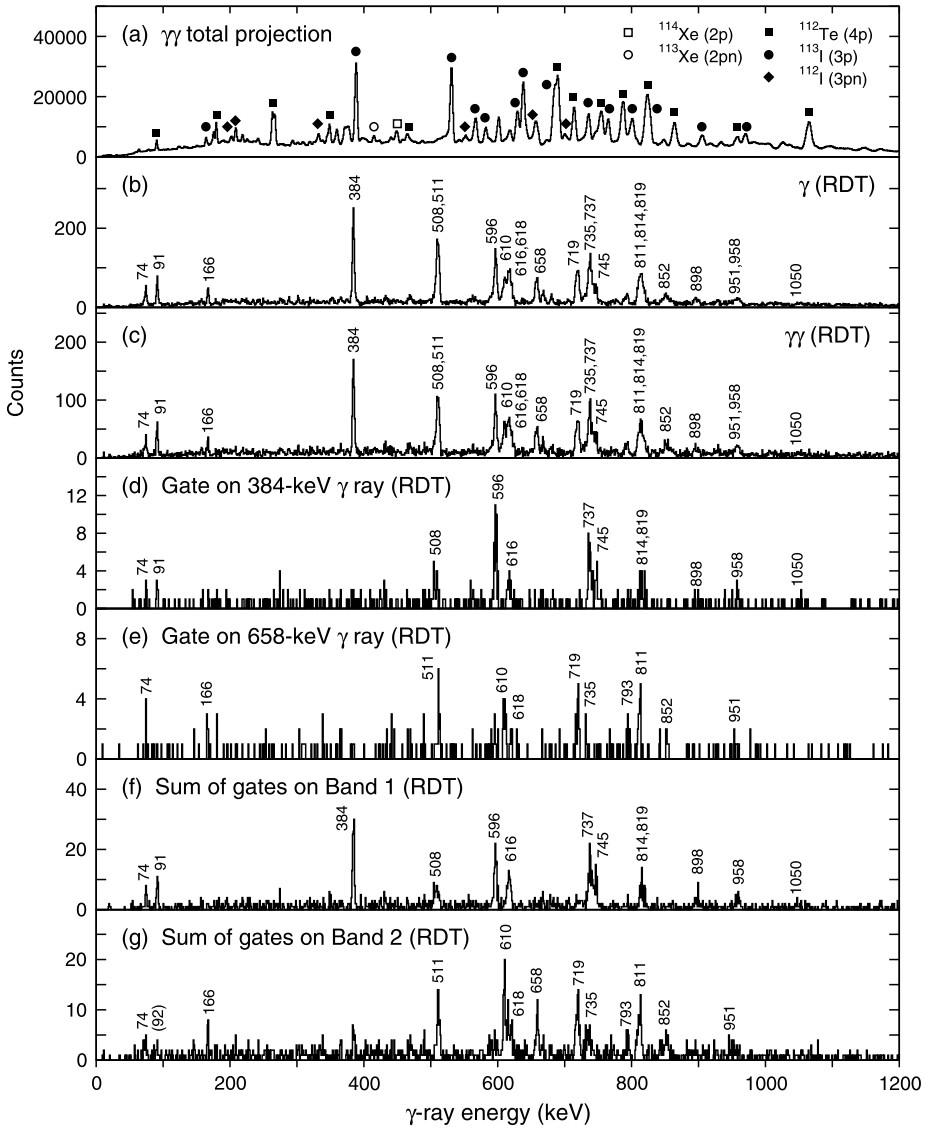

Fig. 2. Gamma-ray spectra recorded in this work. Panel (a) gives the projection of a $\gamma\gamma$ matrix, incremented by all γ rays that are detected in coincidence with an evaporation residue at the focal plane of RITU; the largest peaks in the spectrum correspond to transitions in ^{112}Te ($4p$ evaporation), ^{113}I ($3p$), and ^{112}I ($3pn$). Panels (b) to (g) show γ rays that are tagged with a 969-keV proton being emitted within 100 μs of an implant (RDT gated), in which all of the labelled peaks represent transitions that have been assigned to ^{113}Cs. Panels (b) and (c) show the γ (singles) and $\gamma\gamma$ (doubles) projections, respectively. Panels (d) and (e) show γ rays in coincidence with the 384- and 658-keV γ rays, respectively, revealing different subsets of the ^{113}Cs γ rays. Panel (f) shows γ rays in coincidence with the transitions at 384, 508, 596, 616, or 737 keV; the resulting transitions are assigned to Band 1. Panel (g) shows γ rays in coincidence with the transitions at 511, 658, 719, 811, or 735 keV; the resulting transitions are assigned to Band 2. The presence of the (92)-keV transition in panel (g) is discussed in the text.

identification of the ^{113}Cs residues, the RDT technique was applied. The spectra shown in Figs. 2(b) to (g) show γ rays that are tagged with a 969-keV proton emitted within 100 μs of an implant. With these conditions, Fig. 2(b) shows the associated γ rays (singles) recorded, and Fig. 2(c) shows the total projection of $\gamma\gamma$ data. Figs. 2(d) and (e) show γ rays in coincidence with 384- and 658-keV transitions, revealing coincidence relationships with different subsets of the transitions from panels (b) and (c). Figs. 2(f) and (g) show sums of spectra in coincidence with the subsets of transitions apparent in the gated spectra in panels (d) and (e).

From the spectra shown in Fig. 2, around 20 γ-ray transitions were definitively assigned to ^{113}Cs, along with several tentative transitions. The energies and relative intensities of the transitions are given in Table 1. The uncertainties on energy and intensity are related to the strength of the transition although, for doublet peaks, uncertainties in Gaussian fitting are significant. In order to help determine multipolarities of the transitions, angular-intensity measurements were carried out, at different values of the polar angle θ, where $\theta = 0°$ is the direction of the beam. Intensities at $72° \leq \theta \leq 107°$ ($\theta \approx 90°$) were compared to intensities at $133° \leq \theta \leq 157°$ ($\theta \approx 145°$), and the ratio R of these values $[I(\sim 145°)/I(\sim 90°)]$ was taken. The R values were calibrated using known transitions in ^{113}I and ^{112}Te, giving values of $\sim$0.75 for pure stretched-dipole transitions and $\sim$1.20 for stretched-quadrupole transitions. Values of R are given in Table 1. Although the degree of alignment for the lower-spin states is apparent, most of the transitions assigned to ^{113}Cs have R values consistent with stretched-quadrupole character.

Coincidence relationships and relative intensities, have been used to deduce the level scheme for ^{113}Cs shown in Fig. 3. The level scheme consists of two rotational sequences, labelled Band 1 and Band 2, each of which consists of around ten E2 transitions. Both of the bands are in coincidence with low-energy transitions; Band 1 is in coincidence with transitions at 74 and 91 keV, and

Table 1
Properties of γ rays assigned to ^{113}Cs. The columns labelled E_γ and I_γ give gamma-ray energies and intensities, respectively. R gives the angular-intensity ratios, as defined in the text. The last four rows give transitions in ^{112}Te and ^{113}I which were used to calibrate the values of R.

E_γ (keV)	I_γ	R	ΔI	$I_i^{\pi_i} \rightarrow I_f^{\pi_f}$	Multipolarity
74.1(3)	50(20)	0.5(6)			
91.0(2)	88(8)	1.1(5)			
166.3(2)	10(2)	0.9(6)			
383.9(2)	100(4)	0.97(7)	2	$(11/2^+) \rightarrow (7/2^+)$	E2
508.0(5)	60(6)	1.0(4)	2	$(27/2^+) \rightarrow (23/2^+)$	E2
510.7(3)	60(7)	1.0(1)	2	$(9/2^+) \rightarrow (5/2^+)$	E2
596.2(2)	100(5)	1.03(9)	2	$(15/2^+) \rightarrow (11/2^+)$	E2
610.0(4)	63(6)	1.5(3)	2	$(13/2^+) \rightarrow (9/2^+)$	E2
616.0(4)	51(11)	1.5(4)	2	$(31/2^+) \rightarrow (27/2^+)$	E2
617.9(6)	44(11)	1.4(3)	2	$(29/2^+) \rightarrow (25/2^+)$	E2
658.4(4)	58(5)	1.4(1)	2	$(25/2^+) \rightarrow (21/2^+)$	E2
718.7(4)	80(6)	1.0(2)	2	$(17/2^+) \rightarrow (13/2^+)$	E2
735.1(6)	42(7)	1.1(4)	2	$(33/2^+) \rightarrow (29/2^+)$	E2
737.1(4)	87(7)	1.4(2)	2	$(19/2^+) \rightarrow (15/2^+)$	E2
744.8(5)	48(5)	0.9(3)	2	$(35/2^+) \rightarrow (31/2^+)$	E2
793.3(7)	35(8)	1.8(6)	2	$(37/2^+) \rightarrow (33/2^+)$	E2
811.2(4)	65(13)	1.2(3)	2	$(21/2^+) \rightarrow (17/2^+)$	E2
813.7(5)	65(14)	1.2(2)	2	$(23/2^+) \rightarrow (19/2^+)$	E2
819.2(9)	37(10)	0.4(8)	2	$(39/2^+) \rightarrow (35/2^+)$	E2
852.3(8)	30(5)	3(2)	2	$(41/2^+) \rightarrow (37/2^+)$	E2
897.9(8)	28(4)	1.2(5)	2	$(43/2^+) \rightarrow (39/2^+)$	E2
951(2)	17(6)		2	$(45/2^+) \rightarrow (41/2^+)$	E2
958(1)	22(6)	2(1)	2	$(47/2^+) \rightarrow (43/2^+)$	E2
1050(2)	15(5)		2	$(51/2^+) \rightarrow (47/2^+)$	E2
264		0.73(5)	1	^{113}I	E1
269		0.82(5)	1	^{112}Te	E1
766		1.20(4)	2	^{113}I	E2
864		1.20(4)	2	^{112}Te	E2

Band 2 is in coincidence with transitions at 74 and 166 keV. The 74-keV transition has therefore been placed as the lowest transition in the level scheme, in coincidence with both bands. The level scheme presented here represents a modification of that presented in Ref. [21]; the ordering of the transitions within each sequence has been revised, and the bands have been extended by $\sim$6 $\hbar$ by the observation of several new transitions. In Fig. 3, the lowest states in Bands 1 and 2 have been given spin assignments of X and Y. On the basis of the configuration assignments discussed below, it is proposed that X is 7/2 and Y is 5/2, and that both bands have positive parity. The transitions at 74, 91, and 166 keV have large uncertainties on the R values. A consideration of the energies and total intensities of these transitions suggests that they are likely to predominantly be of M1 character. It is therefore proposed that the 91-keV transition decays from the $7/2^+$ bandhead of Band 1, to a $5/2^+$ state, which subsequently decays to the $3/2^+$ ground state. The 166-keV transition is proposed to decay from the $5/2^+$ bandhead of Band 2 directly to the $3/2^+$ ground state. There is some evidence for a transition with energy close to 91 keV being in coincidence with Band 2, as shown in Fig. 2(g), which could represent the transition from the $5/2^+$ bandhead of Band 2 to the $5/2^+$ state at 74 keV. The $3/2^+$ assignment of the ground state would be consistent with the systematic study of Delion, Liotta, and Wyss in Ref. [30].

It should be noted that the bands observed here extend to spins over 20 $\hbar$ and energies in excess of 8 MeV above the lowest state observed. These are the highest excitation energies and angular momenta observed to date in any nucleus beyond the proton dripline. Prompt proton decay of the excited states would result in a ^{112}Xe recoil which would be excluded from the RDT selection performed here. An attempt has been made to search for ^{113}Cs/^{112}Xe γ-ray coincidences in the recoil-gated prompt γ-ray data, but it is unfortunately not possible to select the ^{113}Cs γ rays by γ-ray gating only, due to the low production cross-section.

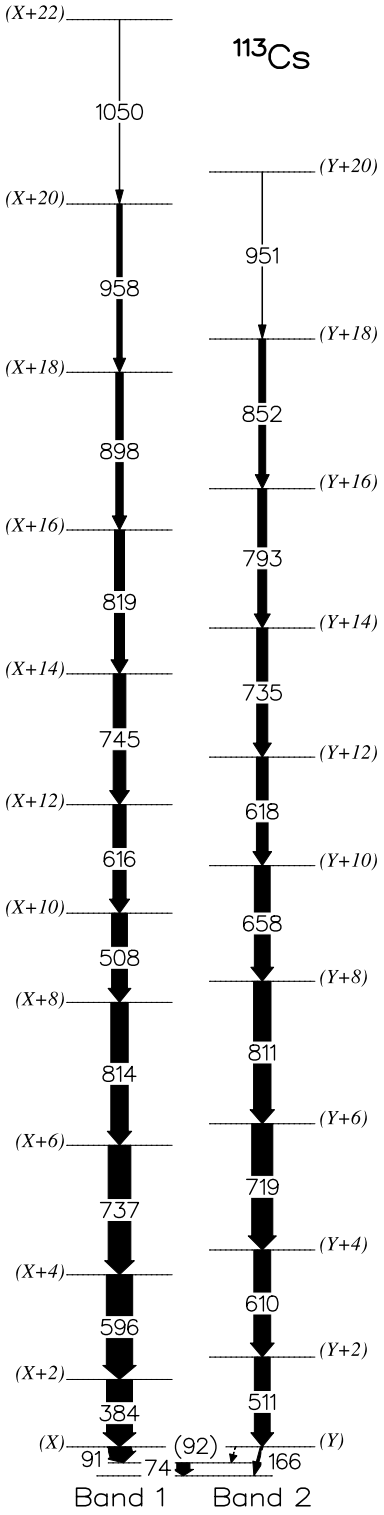

Fig. 3. The level scheme of ^{113}Cs deduced in the present work. The widths of the arrows are proportional to the relative γ-ray intensities. The values in parentheses are spins relative to the lowest state in each band which have been assigned here as X and Y for Bands 1 and 2, respectively. The spin and parity assignments are discussed in the text.

The cesium isotopes with $A \lesssim 125$ are known to be reasonably well deformed ($\beta_2 \simeq 0.20$–0.25) [31] and it is therefore expected that the energies of their excited states will vary smoothly as a function of neutron number. The data for the lower states

Table 2
Orbitals close to the Fermi surface in ^{113}Cs, together with the associated nomenclature (Label).

	Subshell	Nilsson configuration	Label	
		$[Nn_z\Lambda]\Omega^\pi$	$\alpha=-1/2$	$\alpha=+1/2$
Protons	$g_{7/2}$	$[422]3/2^+$	b	a
	$d_{5/2}$	$[420]1/2^+$	d	c
	$h_{11/2}$	$[550]1/2^-$	e	f
	$h_{11/2}$	$[541]3/2^-$	g	h
Neutrons	$d_{5/2}$	$[411]3/2^+$	B	A
	$g_{7/2}$	$[422]3/2^+$	D	C
	$h_{11/2}$	$[550]1/2^-$	E	F
	$h_{11/2}$	$[541]3/2^-$	G	H

Table 3
Deformations of configurations based on proton orbitals in ^{113}Cs. The left-hand column gives the orbital of the proton in the standard nomenclature. The other three columns give the β_2, γ, and β_4 deformation parameters as calculated by total-Routhian surface calculations at a rotational frequency of $\omega=0.192$ MeV/$\hbar$.

$\nu(\alpha,\pi)$	β_2	$\gamma(^\circ)$	β_4
a$(+,+1/2)$	0.205	−1.1	0.041
b$(+,-1/2)$	0.199	0.0	0.036
c$(+,+1/2)$	0.201	+0.8	0.037
d$(+,-1/2)$	0.204	−1.0	0.040
e$(-,-1/2)$	0.214	+6.6	0.044
f$(-,+1/2)$	0.217	−5.4	0.044
g$(-,-1/2)$	0.200	−120.0	0.044
h$(-,+1/2)$	0.219	−2.3	0.045

of the ^{113}Cs bands are in reasonable agreement with the excitation energy systematics of bands in ^{117,119,121,123}Cs [13,18,19]; in particular, the data for Band 2 in ^{113}Cs appear to follow the trends of the $\pi(g_{7/2}d_{5/2})$ bands rather well. Comparison of experimental aligned angular momenta with theoretical predictions, together with the application of blocking arguments, can provide information about the configurations underlying rotational bands. In the present work, a procedure has been adopted whereby Total-Routhian Surface (TRS) calculations [32,33] have been carried out to determine the deformations of likely configurations of the odd proton, following which these deformations were used in Woods–Saxon cranked-shell-model (CSM) calculations [34] to predict properties of the quasiparticle alignments. With $\beta_2=0.207$ [31], the orbitals which lie closest to the Fermi surface are listed in Table 2. The lowest-lying negative-parity proton orbitals are from the $h_{11/2}[550]1/2^-$ subshell (denoted as e and f in the standard nomenclature) and the lowest positive-parity orbitals are from the $g_{7/2}[422]3/2^+$ (a and b) and $d_{5/2}[420]1/2^+$ (c and d) subshells. It should be noted that the a, b, c, and d orbitals are calculated to be closer to the Fermi surface than e and f. TRS-calculated deformations for the likely proton configurations are given in Table 3; it can be seen from this table that the deformations are reasonably constant with $\beta_2\simeq 0.2$, $\beta_4\simeq 0.04$, and $\gamma\simeq 0^\circ$. The only exception is the third negative-parity (g) configuration which has $\gamma=-120^\circ$, but which is not expected to play an important role at low excitation energies.

From previous studies of neighboring nuclei, it is expected that the lowest quasiparticle alignments in ^{113}Cs will be due to pairs of neutrons and protons in $h_{11/2}$ subshells. This expectation is consistent with CSM calculations performed here, where pairs of both $h_{11/2}$ neutrons and protons are predicted to align between ∼0.3 and ∼0.6 MeV/$\hbar$. Quasiparticle Routhians from the CSM calculations are shown in Fig. 4. The alignments of pairs of positive-parity neutrons and protons are not predicted to occur below ∼0.6 MeV/$\hbar$, which is beyond the limit of the observations

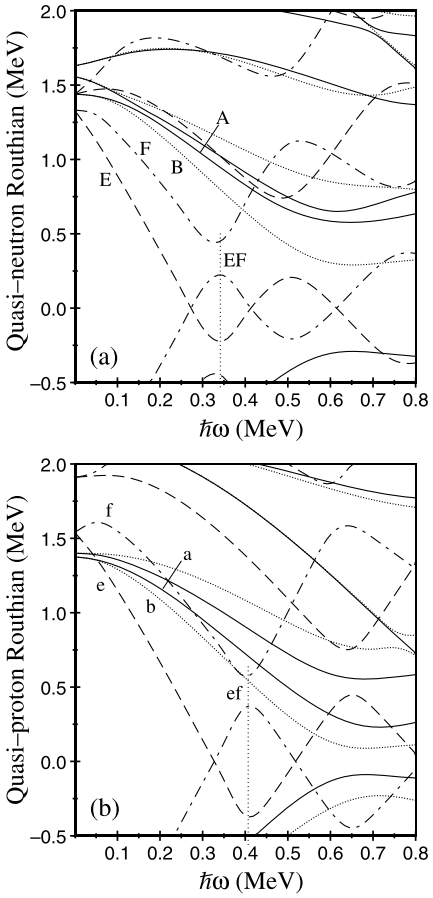

Fig. 4. Quasiparticle Routhians from Woods–Saxon cranked-shell model calculations for (a) neutrons and (b) protons. The calculations are performed for a deformation of $\beta_2=0.20$, $\beta_4=0.04$, and $\gamma=0^\circ$. The different line styles represent values of parity and signature, $(\pi,\ \alpha)$, as follows: dashed lines $(1,-1/2)$; dot-dashed lines $(-,+1/2)$; solid lines $(+,+1/2)$; and dotted lines $(+,-1/2)$. The two lowest negative- and positive-parity quasiparticles, are labelled using the standard nomenclature. The positions of the lowest alignments for neutrons [EF; panel (a)] and protons [ef; panel (b)] are marked by faint vertical dotted lines.

in the present work. Over the range of deformations of the configurations in Table 3, CSM calculations show that there is very little variation in the alignment frequencies of the first and second pairs of $h_{11/2}$ neutrons (labelled as EF and FG) and protons (ef and fg). Thus, the rotational frequencies at which these alignments occur should be very nearly the same in bands based on all of the possible configurations. The CSM calculations predict that the lowest quasiparticle alignment is the EF alignment at a rotational frequency of ∼0.34 MeV/$\hbar$. This is shortly followed by the ef alignment at a frequency of ∼0.4 MeV/$\hbar$. Subsequently, the FG and fg alignments are predicted to occur at rotational frequencies of ∼0.5 and ∼0.6 MeV/$\hbar$, respectively.

Experimental values of the aligned angular momenta (i_x) of the ^{113}Cs bands and some neighboring isotopes have been extracted according to the prescription given in Ref. [35] and are shown in Fig. 5. For all data points, a reference angular momentum with Harris parameters [36] of $\mathcal{J}_0=17.0$ MeV$^{-1}\hbar^2$ and $\mathcal{J}_1=25.8$ MeV$^{-3}\hbar^4$ has been subtracted. Fig. 5(a) shows the i_x data for both ^{113}Cs bands. The behavior of i_x is very similar in both bands, with a sharp backbend at ∼0.35 MeV/$\hbar$, followed by a gradual increase, centered around ∼0.45 MeV/$\hbar$, up to the highest frequencies observed (∼0.55 MeV/$\hbar$). The rotational frequencies at which these features occur are very close to the predictions for EF and ef alignments from the CSM. The similarity in the behavior

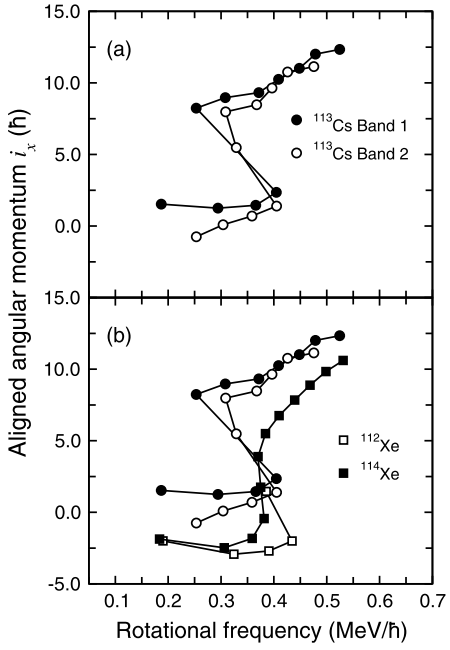

Fig. 5. Aligned angular momenta of the two rotational bands in ^{113}Cs, shown in comparison to neighboring even–even Xe isotopes. For all data points a reference configuration with Harris parameters [36] of $\mathcal{J}_0 = 17.0$ MeV$^{-1}\hbar^2$ and $\mathcal{J}_1 = 25.8$ MeV$^{-3}\hbar^4$ has been subtracted. Panel (a) shows data for both bands in ^{113}Cs. Panel (b) shows the ^{113}Cs data in comparison to the ground-state bands of ^{112,114}Xe. The legend on panel (a) also applies to panel (b). The data for ^{112,114}Xe are taken from Refs. [37,38] and the data for ^{113}Cs are from the present work.

i_x suggests that the two ^{113}Cs bands may be signature partners; however, there is no evidence for any interband transitions, even at the lowest spins. If the bands are not signature partners, then each band consists of a single sequence of E2 transitions, suggesting large signature splitting, characteristic of rotational bands built on a low-Ω orbitals.

Fig. 5(b) shows the i_x values for the ^{113}Cs bands in comparison to the neighboring even–even nuclei ^{112}Xe [37] (the even–even core of ^{113}Cs) and ^{114}Xe [38]. It is clear that the general trend of the i_x data in the even–even nuclei is similar to the bands in ^{113}Cs. In ^{114}Xe a backbend is been observed at 0.4 MeV/$\hbar$ followed by a gradual rise in i_x up to the highest observed rotational frequencies. The similarity of i_x behavior in ^{113}Cs and ^{114}Xe suggests that the same pairs of quasiparticles may be aligning in both nuclei. For ^{114}Xe, in Ref. [38], the backbend at 0.4 MeV/$\hbar$ is assigned to the ef alignment, whereas the gradual upbend that follows is attributed to the EF alignment. The order of the EF and ef alignments in ^{114}Xe is reversed compared to the CSM predictions, but this reversal has also been observed in other nuclei in the region [19,39]. In Ref. [21], it is proposed that Band 1 of ^{113}Cs has an underlying $\pi h_{11/2}$ configuration; in this case, the ef alignment in the band would be blocked. It therefore follows that either the alignments observed in ^{113}Cs and ^{114}Xe do not have the same origins, or that neither band in ^{113}Cs is based on a $\pi h_{11/2}$ configuration. At low rotational frequencies, the difference in i_x between the ^{113}Cs bands and the ^{112,114}Xe bands is, at most, 7/2 $\hbar$ for Band 1 and lower than this for Band 2. These values of the initial alignment are consistent with the ^{113}Cs bands having $\pi g_{7/2}$ or $\pi d_{5/2}$ configurations, but are rather too low for a low-Ω $\pi h_{11/2}$ configuration. For example, even with an $\Omega = 7/2$ $\pi h_{11/2}$ orbital, which is expected to be well above the Fermi level in ^{113}Cs, the initial alignment would be over 4 $\hbar$. The i_x data for ^{113}Cs can also be compared to the neighboring heavier cesium isotopes ^{117,119,121}Cs, which were discussed in Ref. [19]. With decreasing neutron number the first alignment changes from a gradual upbend in ^{121}Cs to a clear backbend in ^{113}Cs. As discussed in Ref. [19], this is likely to be indicative of a reduction in the interaction strength.

Although it is possible to explain the observed alignment properties using traditional CSM calculations, it should be noted here that the effects of neutron–proton (np) correlations have been shown to influence alignment properties close to $N = Z$. In Ref. [40], the traditional CSM mean-field approach was extended to include isovector np pairing in nuclei near $N = Z$, and such calculations were able to properly describe the alignments in $N \simeq Z$, $A \simeq 70$ nuclei. In Ref. [41], shell-model calculations were performed for high-j intruder orbitals, which suggested that, for prolate deformations, the alignment of one type of particles in a high-j shell is delayed when the other type of particles is present in the same high-j shell. This delay is expected to be maximized for $N = Z$. Thus, for ^{113}Cs, with $N = Z + 3$ and with the Fermi level for neutrons in the low-Ω $h_{11/2}$ orbitals, it can be expected that $\pi h_{11/2}$ alignment, in the presence of $h_{11/2}$ neutrons, will be affected by np correlations. Although it is explicitly stated in Ref. [41] that the results of the calculations should not be compared with experimental data quantitatively, until they have been performed with a more realistic shell-model configuration space, it is likely that np correlations will play a role in ^{113}Cs, and it would be very interesting to explore this aspect further.

Considering the evidence discussed above, it is proposed here that both of the observed bands have positive parity, with Band 1 being based on the [422]3/2$^+$ $g_{7/2}$ orbital and Band 2 based on the [420]1/2$^+$ $d_{5/2}$ orbital. The ordering of the observed alignments is not clear from the present data. Calculations suggest that the first backbend at ∼0.35 MeV/$\hbar$ is due to EF alignment, and the upbend at ∼0.45 MeV/$\hbar$ is due to the ef alignment. However, in positive-parity bands in the heavier neighboring ^{117,119,121}Cs [19], and other neighboring nuclei such as ^{114}Xe, the order of these alignments is reversed. The similarity in the i_x behavior of the two ^{113}Cs bands would seem to make it unlikely that one of the bands is based on a negative-parity ($\pi h_{11/2}$) proton orbital, with the other based on a positive-parity ($\pi d_{5/2}/g_{7/2}$) proton orbital. It cannot be ruled out, however, that both bands are based on $\pi h_{11/2}$ orbitals, with the alignment frequencies shifted from the values calculated by traditional CSM calculations. Presently, however this seems to be less likely than the positive-parity assignments that are proposed.

In summary, high-spin spectroscopy of the proton-emitting nucleus ^{113}Cs has been performed using the recoil-decay tagging method. Over 20 γ-ray transitions have been assigned to ^{113}Cs by correlation with characteristic ^{113}Cs proton decays. The ^{113}Cs proton-decay energy and half-life have been measured to be 969(8) keV and 17.1(2) µs, in agreement with previous work. Two previously identified rotational bands have been observed. Transitions in the bands have been rearranged in comparison to previous work, and both bands have been extended to higher spins (tentatively, Band 1 to 51/2$^+$ and Band 2 to 45/2$^+$). A study of aligned angular momenta is consistent with the lowest $\nu h_{11/2}$ and $\pi h_{11/2}$ alignments occurring in both bands. If this is the case, then neither band can be based on a $\pi h_{11/2}$ configuration. It is then proposed that Band 1 is based on the $\pi g_{7/2}[422]3/2^+$ configuration and Band 2 is based on the $\pi d_{5/2}[420]1/2^+$ configuration. The effects of np pairing correlations on the properties of rotational alignments in the high-j $h_{11/2}$ subshell are expected to be significant, and this aspect needs theoretical attention. In order to confirm the interpretation proposed here, a search for the $\pi h_{11/2}$ band in ^{113}Cs would be of significant interest. It should also be noted here that a study of excited states in ^{115}Cs, for which there are presently no experimental data, would help trace the evolution of structure in the cesium isotopes across the proton drip line.

Acknowledgements

The following support is acknowledged: Science and Technology Facilities Council (UK) (grant ST/J000183/2); EURONS, the I3-TNA project of EU FP6 (Contract 506065); the Centre of Excellence programme of the Academy of Finland (Contract 213503); and Gammapool, for the loan of the Jurogam HPGe detectors.

References

[1] R. Kirchner, et al., Phys. Lett. B 70 (1977) 150.
[2] J.M. D'Auria, et al., Nucl. Phys. A 301 (1978) 397.
[3] P.O. Larsson, et al., Z. Phys. A 314 (1983) 9.
[4] T. Faestermann, et al., Phys. Lett. B 137 (1984) 23.
[5] A. Gillitzer, et al., Z. Phys. A 326 (1987) 107.
[6] R.D. Page, et al., Phys. Rev. Lett. 72 (1994) 1798.
[7] J.M. Batchelder, et al., Phys. Rev. C 57 (1998) R1042.
[8] K.-H. Schmidt, et al., Phys. Lett. B 168 (1986) 39.
[9] R.S. Simon, et al., Z. Phys. A 325 (1986) 197.
[10] E.S. Paul, et al., Phys. Rev. C 51 (1995) 78.
[11] P. Rahkila, et al., Phys. Rev. C 82 (2010) 011303.
[12] C.-B. Moon, et al., J. Korean Phys. Soc. 38 (2001) 83.
[13] Kuljeet Singh, et al., Eur. Phys. J. A 25 (2005) 345.
[14] J.R. Hughes, et al., Phys. Rev. C 44 (1991) 2390.
[15] Y. Liang, et al., Phys. Rev. C 42 (1990) 890.
[16] S. Sihotra, et al., Phys. Rev. C 79 (2009) 044317.
[17] S. Sihotra, et al., Phys. Rev. C 78 (2008) 034313.
[18] A.M. Hurst, M.Sc. thesis, University of Manchester, 2003.
[19] J.F. Smith, et al., Phys. Rev. C 63 (2001) 024319.
[20] C. Gross, et al., in: Proceedings of the Conference on Exotic Nuclei and Atomic Masses, ENAM 1998, in: AIP Conference Proceedings CP, vol. 455, 1998, p. 444.
[21] C.-H. Yu, et al., in: Proceedings of Proton-Emitting Nuclei, PROCON 2003, in: AIP Conference Proceedings CP, vol. 681, 2003, p. 172.
[22] P.J. Nolan, Nucl. Phys. A 520 (1990) 657c.
[23] M. Leino, et al., Nucl. Instrum. Methods Phys. Res., Sect. B, Beam Interact. Mater. Atoms 99 (1995) 653.
[24] R.D. Page, et al., Nucl. Instrum. Methods Phys. Res., Sect. B, Beam Interact. Mater. Atoms 204 (2003) 634.
[25] I. Lazarus, et al., IEEE Trans. Nucl. Sci. 48 (2001) 567.
[26] M.P. Waring, et al., Phys. Rev. C 51 (1995) 2427.
[27] H.C. Scraggs, et al., Phys. Rev. C 61 (2000) 064316.
[28] P.J. Sellin, et al., Phys. Rev. C 47 (1993) 1933.
[29] R.D. Page, et al., Phys. Rev. C 49 (1994) 3312.
[30] D.S. Delion, R.J. Liotta, R. Wyss, Phys. Rev. Lett. 96 (2006) 072501.
[31] P. Möller, J.R. Nix, W.D. Myers, W.J. Swiatecki, At. Data Nucl. Data Tables 59 (1995) 185.
[32] R. Wyss, J. Nyberg, A. Johnson, R. Bengtsson, W. Nazarewicz, Phys. Lett. B 215 (1988) 211.
[33] W. Nazarewicz, R. Wyss, A. Johnson, Nucl. Phys. A 503 (1989) 285.
[34] W. Nazarewicz, J. Dudek, R. Bengtsson, T. Bengtsson, I. Ragnarsson, Nucl. Phys. A 435 (1985) 397.
[35] R. Bengtsson, S. Frauendorf, Nucl. Phys. A 327 (1979) 139.
[36] S.M. Harris, Phys. Rev. B 138 (1965) 509.
[37] J.F. Smith, et al., Phys. Lett. B 523 (2001) 13.
[38] E.S. Paul, et al., Nucl. Phys. A 673 (2000) 31.
[39] R. Wyss, et al., Nucl. Phys. A 503 (1989) 244.
[40] Stefan G. Frauendorf, Javid A. Sheikh, Nucl. Phys. A 645 (1999) 509.
[41] S. Frauendorf, J.A. Sheikh, Phys. Rev. C 59 (1999) 1400.